Nuclear effects in atomic spectra

- Search for metastable isotopes of superheavy elements (island of stability)
- King plot for isotope shift and search for new physics
- High sensitivity to shape of nuclei due to large relativistic effects in heavy atoms (effects beyond change of nuclear radius)
- Effects of nuclear polarization in atomic spectra

- Slides made by V.A. Dzuba, A.V. Viatkina, H.B. Tran Tan, P. Munro-Laylim

Isotope shift and search for island of stability.

Super Heavy Elements (SHE) produced in labs are always neutron deficient and highly unstable. Proton repulsion grows as ***Z^2***; N must grow faster than ***Z*** to compensate. Therefore, ***N/Z*** is larger in **SHE** than in lighter elements.

E.g., the heaviest synthetic isotope of flerovium (magic proton number ***Z=114***) is produced in the reaction

$$^{244}_{94}\mathrm{Pu} + ^{48}_{20}\mathrm{Ca} \rightarrow ^{292}_{114}\mathrm{Fl}^* \rightarrow ^{290}_{114}\mathrm{Fl} + 2^1_0 n$$

It is **8** neutrons short of magic neutron number ***N=184***.

$^{298}_{114}\mathrm{Fl}$ is a candidate for the island of stability; lifetime ≈ 10^7yr ?

We suggest to search for stable SHE in astrophysical data, focusing on events which ensure huge influx on neutrons, e.g. supernova explosion, neutron star/black hole mergers. **If we add calculated isotope shifts to measured atomic spectra of neutron-deficient isotope produced in laboratory,** $E=E_0 + IS$, **we predict spectra of neutron-rich isotopes near island of stability which may be searched in astrophysical data.** Spectra of Es Z=99 from a star observed (?)

Three steps

- Measure the frequencies of E1 transitions in available neutron-poor isotopes.
- Calculate isotope shift to expected island of stability nuclei (neutron numbers close to magic N=184) and add it to the measured frequencies.
- Search for these spectral lines in astrophysical data.

Dzuba, Flambaum, Webb, PRA 95, 062515 (2017).
Flambaum,Geddes,Viatkina, PRA 97, 032510 (2018)

Nobelium: the heaviest element with known frequency of an E1 transition.

$$^{254}_{102}\mathrm{No}, \quad \hbar\omega(^1\mathrm{S}_0 -^1\mathrm{P}^o_1) = 29961.457\ \mathrm{cm}^{-1}$$

Laatiaoui et al, Nature (London) **538**, 495 (2016).

Calculating isotope shift and using nuclear data from Agbemava et al, PRC **89**, 054320 (2014) leads to IS = -5.27 cm^{-1} (to N=184), therefore for

$$^{286}_{102}\mathrm{No}, \quad \hbar\omega(^1\mathrm{S}_0 -^1\mathrm{P}^o_1) = 29956.19\ \mathrm{cm}^{-1}$$

This value can be used in astrophysical searches

We have done calculations for other SHE. Dzuba et al, Allehabi et al

King plot for isotope shifts: high sensitivity to nuclear shape and new interactions

King plot for Isotope shift

Standard approach. F-field shift, K- mass shift constants, $\mu = \frac{1}{M_1} - \frac{1}{M_2}$

If we have two lines and

$$\nu_a = F_a \delta \langle r^2 \rangle + K_a \mu$$

$$\nu_b = F_b \delta \langle r^2 \rangle + K_b \mu$$

then

$$\tilde{\nu}_a = \frac{F_a}{F_b} \tilde{\nu}_b - \frac{F_a}{F_b} K_b + K_a \qquad \tilde{\nu} = \nu / \mu$$

points for different isotopes are on the straight line on the $(\tilde{\nu}_a, \tilde{\nu}_b)$ plane (King plot)

King plot for isotope shifts

$$n_{2,AA'} = K_2 + \frac{F_2}{F_1}(n_{1,AA'} - K_1)$$

A, A_1, A_2, A_3 - isotopes of an element Z

- straight line on the $n_1=\nu_1/\mu$, $n_2=\nu_2/\mu$ plane

$$\mu = \frac{1}{M_1} - \frac{1}{M_2}$$

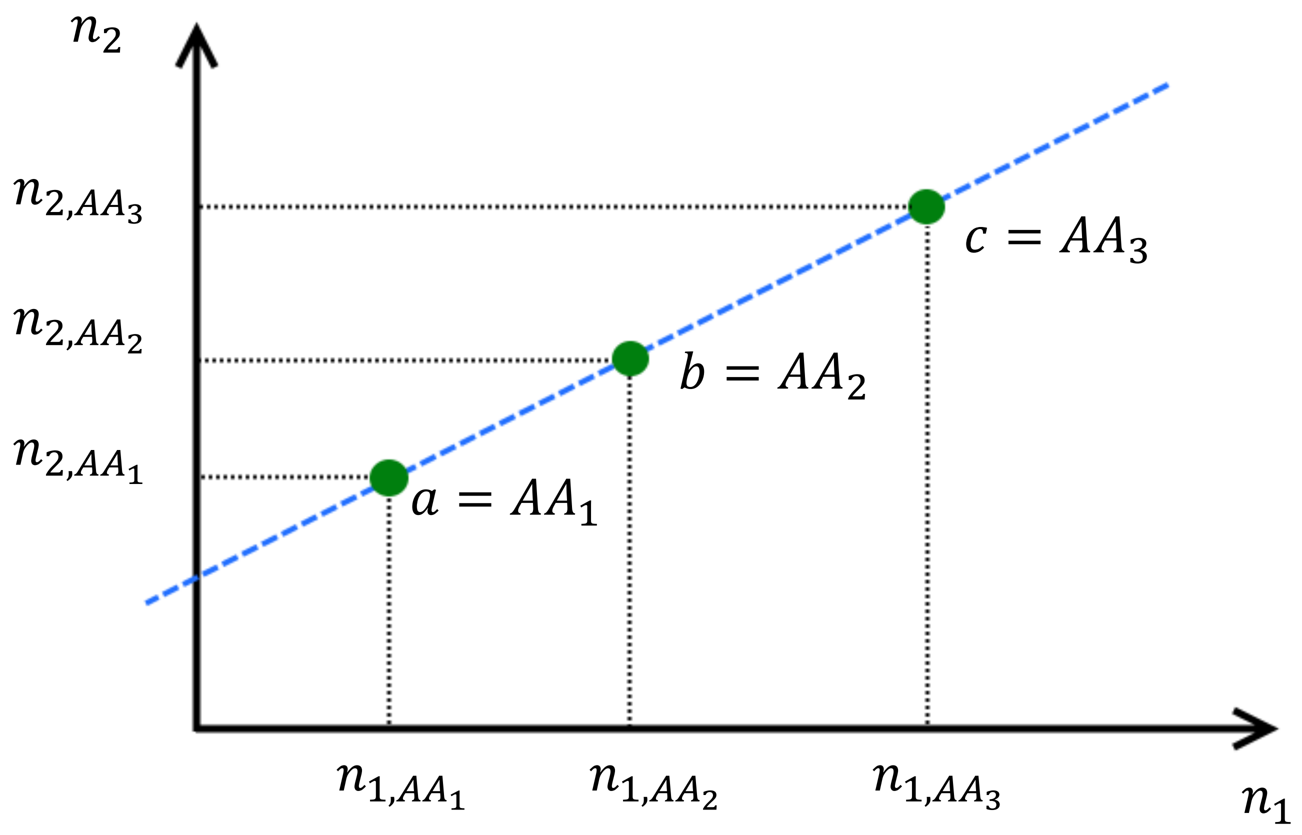

King plot non-linearity

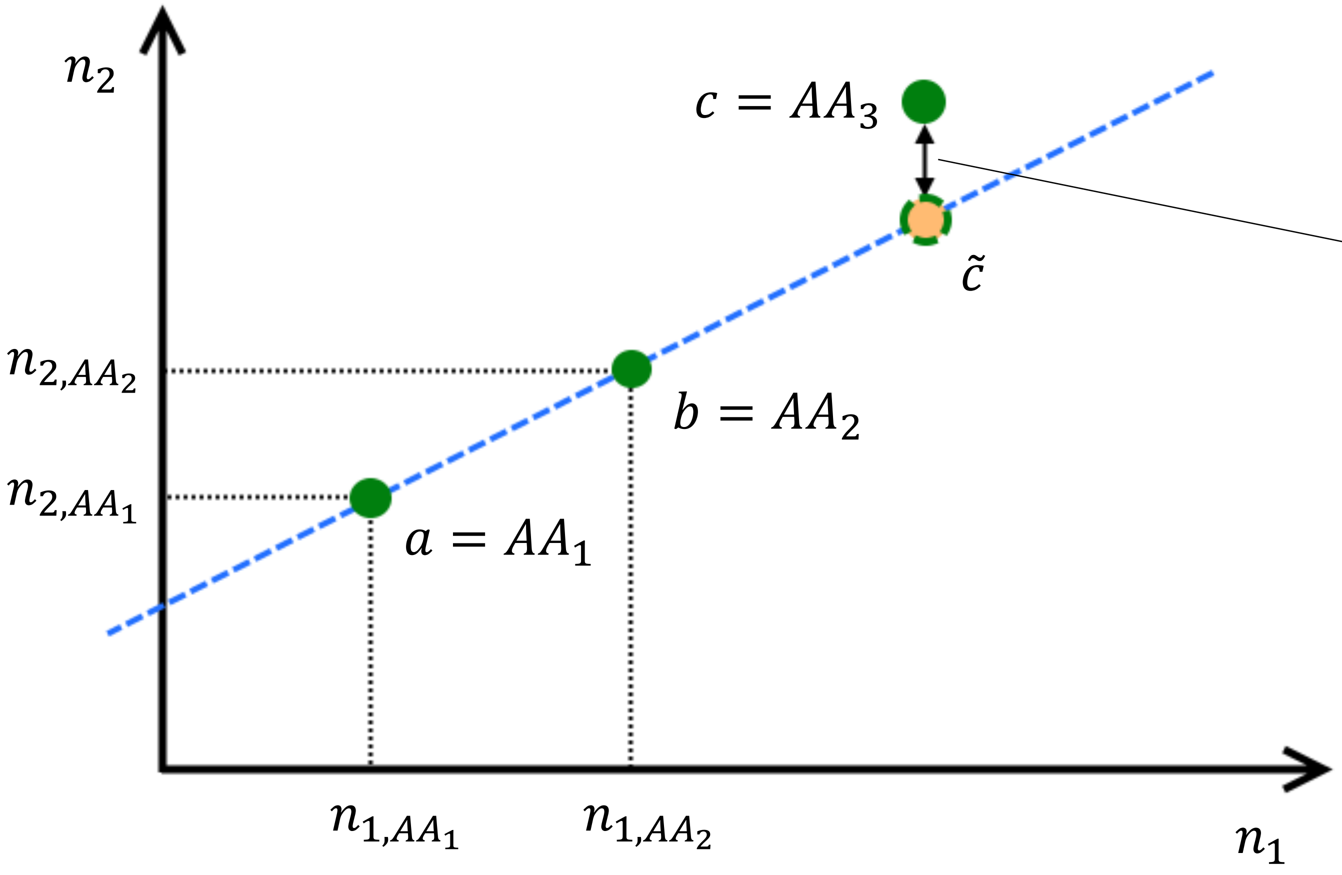

- **New Physics ?!?**

or

- **Nonlinearities from higher-order Standard Model contributions ?**

Search for new interactions using King plot

New interaction breaks linearity. **Berengut et al** Phys. Rev. Lett. 20, 103202, 2018

Yukawa potential produced by scalar particle exchange:

$$V_\varphi = -q_e q_n N \frac{e^{-kr}}{r} \qquad k = \frac{m_\varphi c}{\hbar}$$

Particle's coupling **to electron** **to neutron**

Energy shift:

$$\delta E_{NP} \approx -q_e q_n \Delta N \int_0^\infty \rho_\kappa(r) \frac{e^{-kr}}{r} r^2 dr$$

Electron wave function density

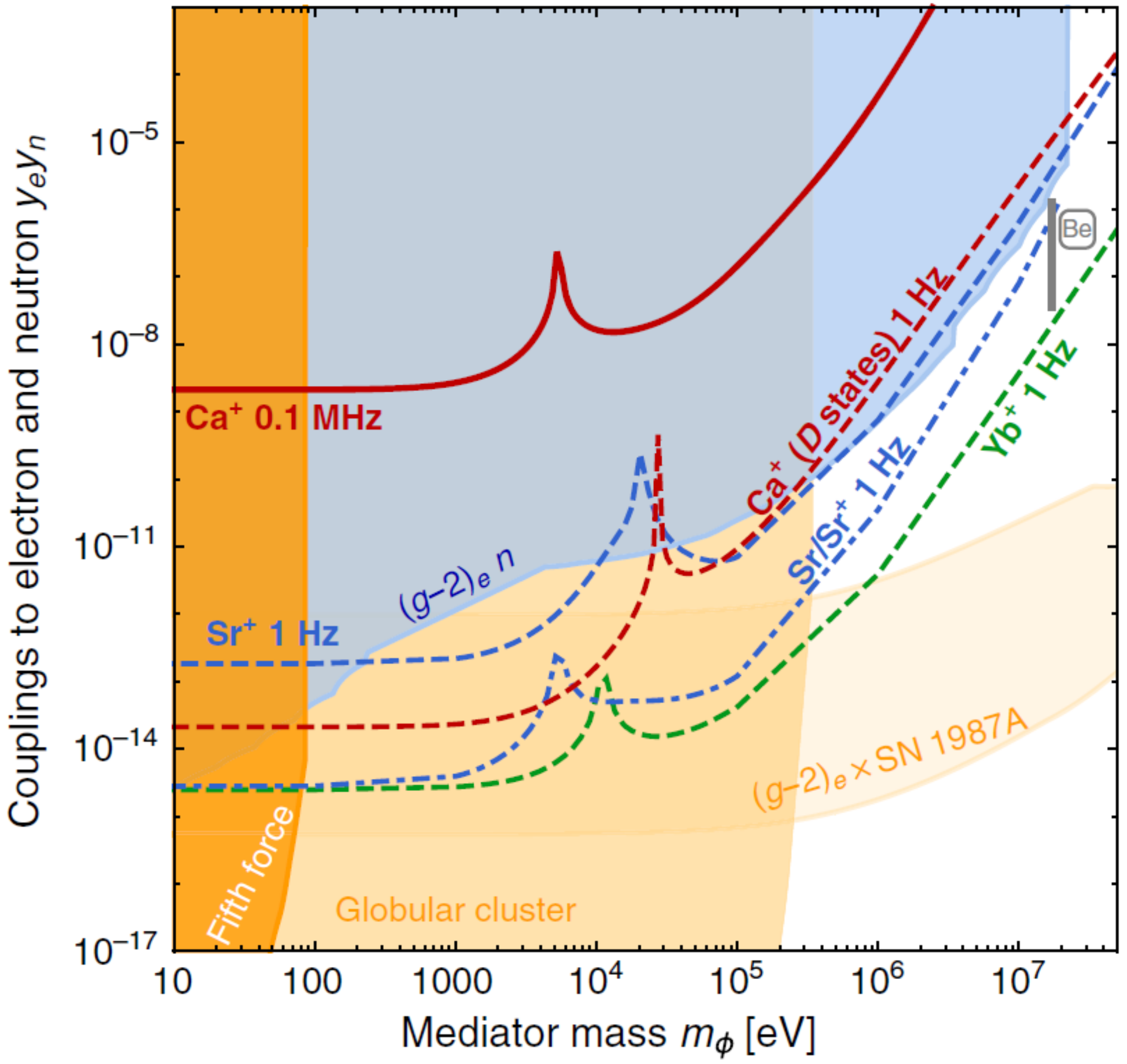

Berengut et al. (2018) *PRL*, 120(9), 091801.   There are several new papers with non-zero nonlinearity in Yb+ and Yb

Gravitational potential in extra dimensions

$$V(r) = \begin{cases} -\dfrac{Gm_1m_2}{r} & \text{for } r \gg R \\ -\dfrac{Gm_1m_2R^n}{r^{n+1}} & \text{for } r \ll R \end{cases}$$

$$\left(\frac{cM_{Pl}}{\hbar}\right)^2 = R^n \left(\frac{cM}{\hbar}\right)^{n+2}$$

R is size of extra spatial dimensions
n is number of extra spatial dimensions
M_{Pl} is observed three-dimensional Planck mass
M is higher dimensional Planck mass
In *n+3* dimensions, gravitational strength is comparable to other interactions

Model
Arkani-Hamed, Dimopoulos, Dvali
Physics Letters B 429 (1998)
[arXiv:hep-ph/9803315]

Effects in atomic spectroscopy
Dzuba, Flambaum, Munro-Laylim
[arXiv:2208.10125]

Neutrino-exchange potential

$$V(r) = \frac{2G_F^2 m^4}{3\pi^3 r} I(r)\left(a_1 a_2 - b_1 b_2\left[\frac{3}{2}\boldsymbol{\sigma_1}\cdot\boldsymbol{\sigma_2} - \frac{5}{2}(\boldsymbol{\sigma_1}\cdot\hat{\boldsymbol{r}})(\boldsymbol{\sigma_2}\cdot\hat{\boldsymbol{r}})\right]\right)$$

$$I(r) = \int_1^\infty e^{-2xmcr/\hbar}\left(x - \frac{1}{4}\right)\frac{\sqrt{x^2-1}\,z^4}{(x^2+z^2)^2}\,dx$$

Dirac neutrinos

$$I(r) = \int_1^\infty e^{-2xmcr/\hbar}\,\frac{(x^2-1)^{3/2} z^4}{(x^2+z^2)^2}\,dx$$

Majorana neutrinos

Interaction has been introduced by
Gamow & Teller
Feynman
Feinberg & Sucher

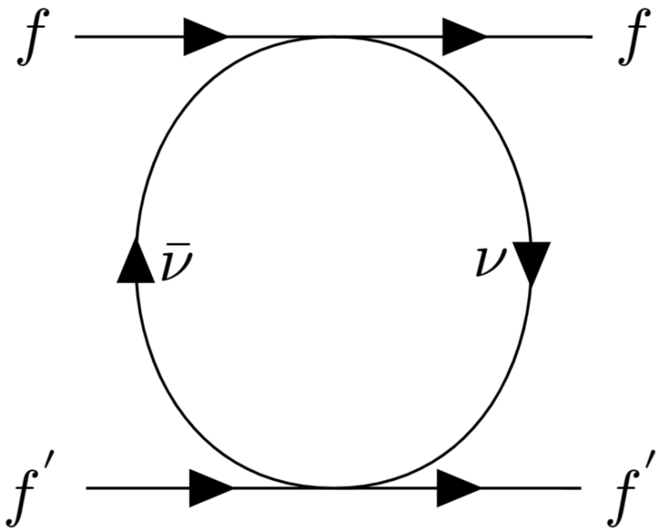

Effects in atomic spectroscopy
Stadnik
PRL 120 223202 (2018)

Munro-Laylim, Dzuba, Flambaum
[arXiv:2207.07325]
+ extension to small distance

Standard Model sources of non-linearity

$$\nu_a^{\mathrm{FS}} = F_a \delta\langle r^2\rangle + G_a^{(2)} \delta\langle r^2\rangle^2 + G_a^{(4)} \delta\langle r^4\rangle$$

The term with ***G***$^{(2)}$ is the second-order correction where perturbation is the change of nuclear potential between isotopes: $\delta V_N = V_N(A_1) - V_N(A_2)$

$$G_a^{(2)} = \sum_n \frac{\langle a|\delta\tilde{V}_N|n\rangle^2}{E_a - E_n} / \delta\langle r^2\rangle^2$$

The term with ***G***$^{(4)}$ contains relativistic and nuclear shape corrections. Dirac electron wave function varies inside the nucleus making the shift sensitive to nuclear charge distribution. Very sensitive test of nuclear models predicting variation of nuclear deformation between isotopes.

Deviation from strait line in King plot for Yb^{+}

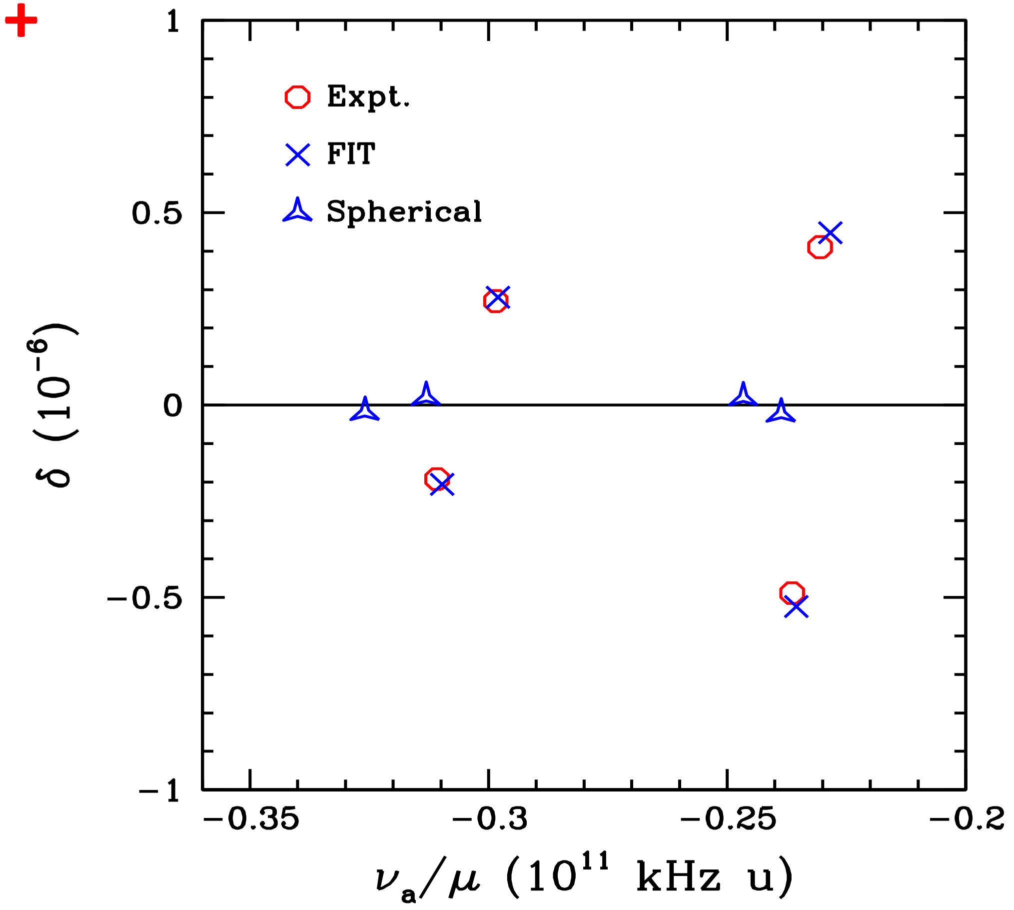

Deviations from straight line

Expt: (Counts et al, PRL **125**, 123002 (2020)).

FIT nuclear model

A	r_p	β
168	5.2950	0.3100
170	5.3080	0.3184
172	5.3202	0.3232
174	5.3297	0.3208
176	5.3387	0.3156

r_p is nuclear RMS radius
β is deformation parameter

Fitting:

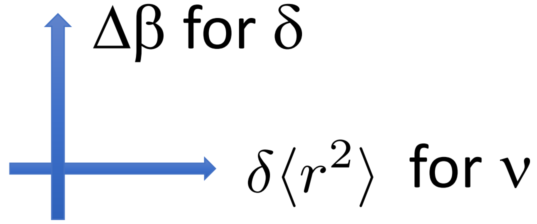

Results of ab initio nuclear calculations

The **FIT** parameters are similar to predictions of the nuclear **C**ovariant **D**ensity **F**unctional **T**heory

S. O. Allehabi, V. A. Dzuba, V. V. Flambaum, A. V. Afanasjev, S. E. Agbemava, Phys. Rev. C 102, 024326 (2020); Phys. Rev. A103, L030801, (2021).

DD-MEδ		DDPC1		FIT	
r_c	β	r_c	β	r_c	β
5.28820	0.33400	5.29528	0.33790	5.2950	0.3100
5.30106	0.33070	5.31318	0.34540	5.3081	0.3184
5.31138	0.32024	5.32346	0.33429	5.3204	0.3232
5.32356	0.31447	5.33291	0.32152	5.3300	0.3208
5.33228	0.30413	5.34420	0.31398	5.3391	0.3156

Conclusion: King plot in heavy atoms

- Dirac electron wave function varies significantly inside heavy nuclei. This introduces field shift which can not be reduced to variation of nuclear radius. We need at least two parameters, radius and deformation, to describe experimental data. This leads to the King plot non-linearity, which is sensitive to nuclear interaction models predicting distribution of nuclear charge.

Nuclear polarization effects in atoms and ions

V. V. Flambaum, I. B. Samsonov, H. B. Tran Tan, and A. V. Viatkina

Phys. Rev. A ***103***, *032811 (2021)*

UNSW SYDNEY

HIM Helmholtz-Institut Mainz

JG|U JOHANNES GUTENBERG UNIVERSITÄT MAINZ

- Isotope shift King's plot nonlinearity → new boson.
- Need to account for all Standard model nonlinearity.
- One source of nonlinearity: nuclear polarization effect.

V.V. Flambaum, A. Geddes, A.V. Viatkina, PRA 97, 032510 (2018)

- <u>Enhanced in heavy atoms/ions:</u> electrons move faster than the nuclear rotation → don't see an 'averaged' nucleus.

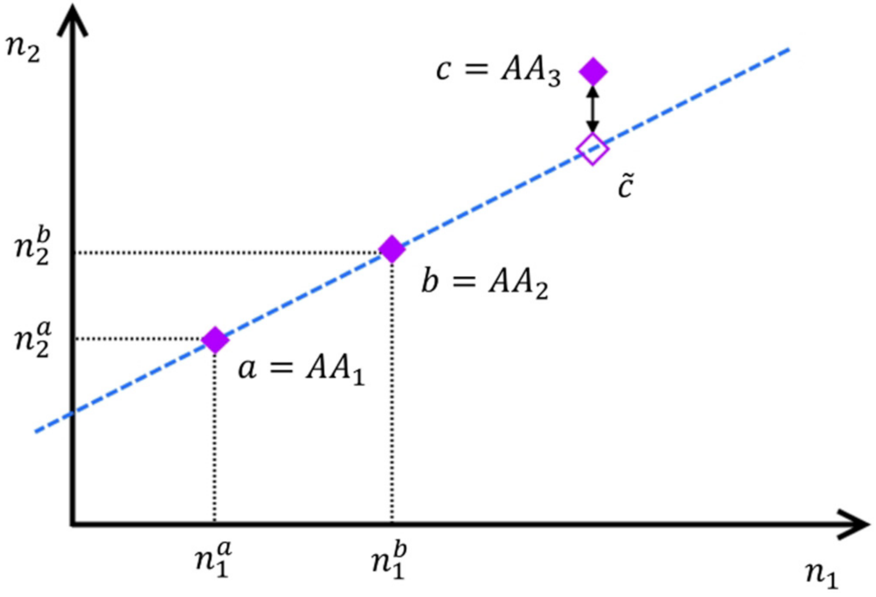

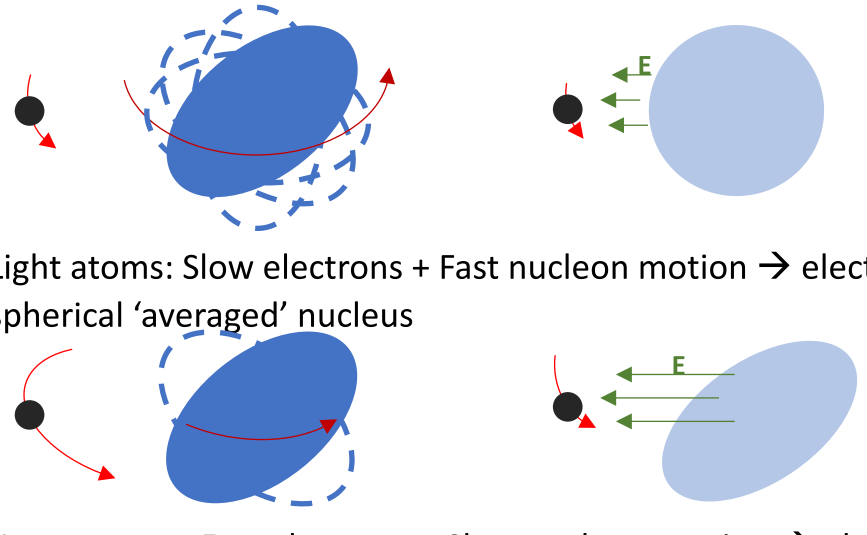

Light atoms: Slow electrons + Fast nucleon motion → electrons see spherical 'averaged' nucleus

Heavy atoms: Fast electrons + Slow nuclear rotation → electrons still see deformed nucleus → large corrections to to the average field approximation

Nuclear polarization effect

- Correction to electron self energy – Lamb shift.
- Due to two-photon interaction with nucleons.

$$\Delta E_{\eta I} = -\tfrac{1}{2}\alpha_{ij}\mathcal{E}_i\mathcal{E}_j$$

$$\alpha_{ij} \equiv -2 \sum_{\eta' I' M'} \frac{\langle \eta I M | d_i | \eta' I' M' \rangle \langle \eta' I' M' | d_j | \eta I M \rangle}{E_{\eta I} - E_{\eta' I'}}.$$

Nuclear polarization effect – Previous works

- K. Pachucki, D. Leibfried & T. W. Hansch, PRA 48, R1 (1993),
  K. Pachucki, M. Weitz & T. W. Hansch, PRA 49, 2255 (1994) → **hydrogen and deuterium.**
- G. Plunien, B. Muller, W. Greiner & G. Soff, PRA 39, 5428 (1989),
  G. Plunien, B. Muller, W. Greiner & G. Soff, PRA 43, 5853 (1991),
  G. Plunien & G. Soff, PRA 51, 1119 (1995),
  G. Plunien & G. Soff, PRA 53, 4614 (1996),
  A. V. Neodov, L. N. Labzowsky, G. Plunien & G. Soff, PLA 222, 227 (1996) → **few heavy, single electron hydrogen-like ions.**
- **Our work:** all atoms and ions, any number of electrons, nuclear charge Z, A → important for actinides and superheavy elements, and King plots for isotope shifts with neutral or singly charged ions (needed to search for new interactions and elementary particles).

Different contributions

- Simultaneous nuclear and electron transitions
- Electronic transitions to discrete spectrum: nlj → n'l'j' → nlj. Small matrix element + large nuclear energy denominator → suppressed.

- Electronic transition to continuum: nlj → ±εj → nlj (continuum intermediate). Both upper and lower continuum contribute since nuclear energy > $m_e c^2$.

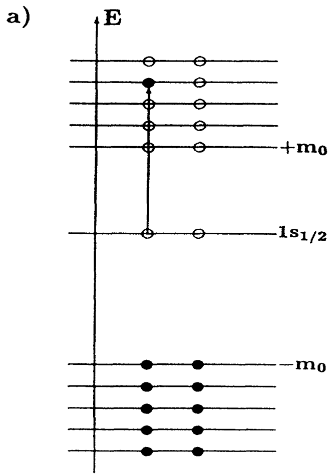

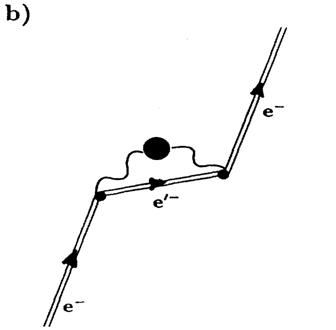

Upper continuum and discrete states contribution

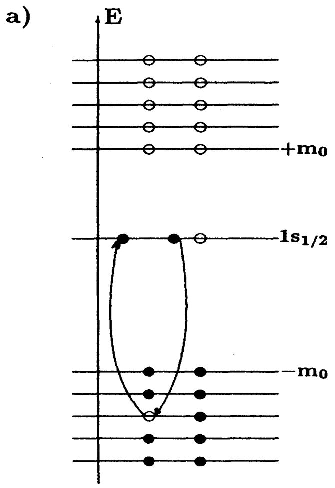

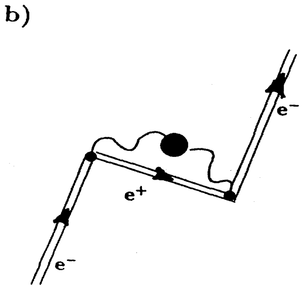

Lower continuum blocking contribution

Giant electric dipole resonance contribution

- Low L transitions have larger overlap with nucleus → larger contribution.
- L=1 → giant electric dipole resonance has very large nuclear matrix elements.

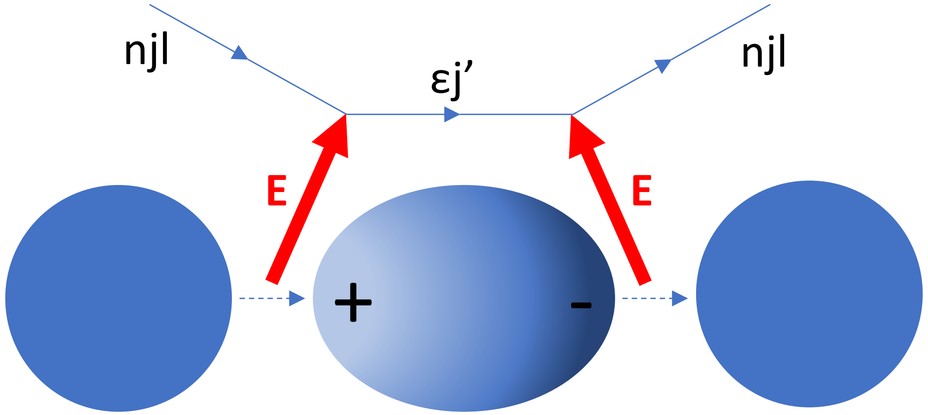

$$\Delta\varepsilon_{nlj} = -\frac{3\alpha}{4\pi}B(E1)\sum_{j'}(2j'+1)\begin{pmatrix} j' & j & 1 \\ \frac{1}{2} & -\frac{1}{2} & 0 \end{pmatrix}^2$$

$$\times\left(\int_{-\infty}^{-m_e}\frac{|\langle nlj|F_1|\varepsilon j'\rangle|^2 d\varepsilon}{\varepsilon-\varepsilon_{nlj}-E_{\mathrm{GR}}} + \int_{m_e}^{\infty}\frac{|\langle nlj|F_1|\varepsilon j'\rangle|^2 d\varepsilon}{\varepsilon-\varepsilon_{nlj}+E_{\mathrm{GR}}}\right),$$

$$E_{\mathrm{GR}} = 95(1-A^{-1/3})A^{-1/3}\ \mathrm{MeV}.$$

$$B(E1) \equiv B(E1;1\to 0) = \frac{3}{8\pi}\frac{Z(A-Z)e^2}{AE_{\mathrm{GR}}m_p}.$$

Giant electric dipole contribution - Results

- Fitting function:

$$\Delta\varepsilon(Z,\Delta A) = -[\exp(a_0 + a_1 Z + a_2 Z^2) Z^{a_3} + \exp(b_0 + b_1 Z + b_2 Z^2) Z^{b_3} \Delta A]\ \text{meV},$$

$$A = A_0(Z) + \Delta A.$$

- Radius variation:

$$\Delta\varepsilon(Z,A,R) = \Delta\varepsilon(Z,A,R_0) + \delta_R\varepsilon(Z)\delta R,$$

$$\delta_R\varepsilon(Z) = \exp(c_0 + c_1 Z + c_2 Z^2) Z^{c_3}\ \text{meV/fm}.$$

	$1s$	$2s$	$2p_{1/2}$
a_0	-22.2	-24.4	-36.3
a_1	-2.21×10^{-2}	-2.36×10^{-2}	-2.92×10^{-2}
a_2	3.07×10^{-4}	3.66×10^{-4}	4.40×10^{-4}
a_3	5.64	5.67	7.80
b_0	-19.9	-22.0	-33.5
b_1	4.23×10^{-3}	3.44×10^{-3}	4.41×10^{-3}
b_2	1.77×10^{-4}	2.32×10^{-4}	2.82×10^{-4}
b_3	3.56	3.57	5.52
c_0	-24.0	-26.2	-38.1
c_1	-1.70×10^{-2}	-1.94×10^{-2}	-2.56×10^{-2}
c_2	3.39×10^{-4}	4.02×10^{-4}	4.75×10^{-7}
c_3	5.44	5.49	7.63

Fitting + computation error < 12%

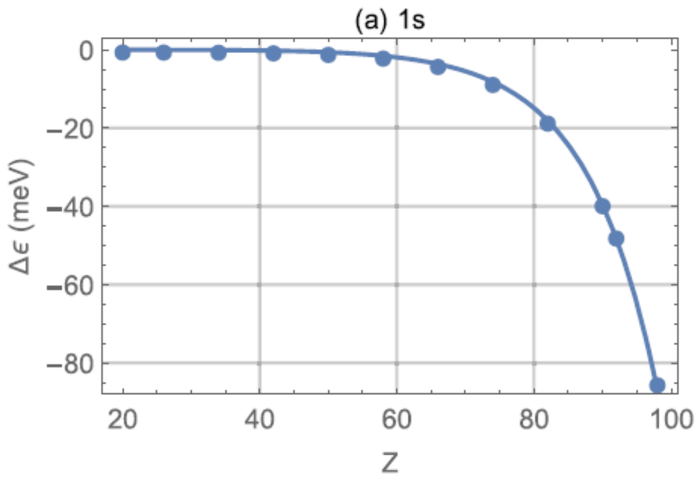

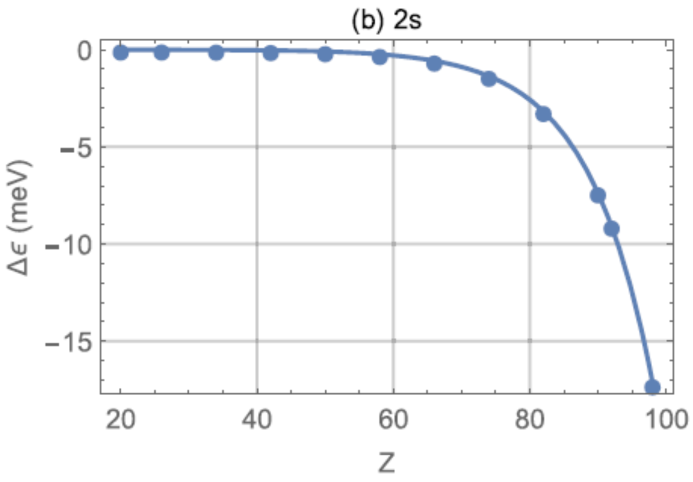

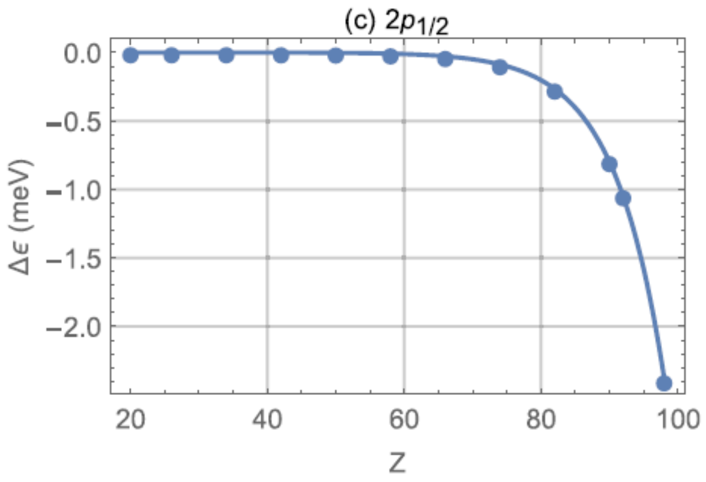

Electric quadrupole contribution

- L=2 nuclear transition → into rotational band is largest ← smallest energy denominator.
- Depend on β_2 (deformation parameter)→ strong King plot nonlinearity.

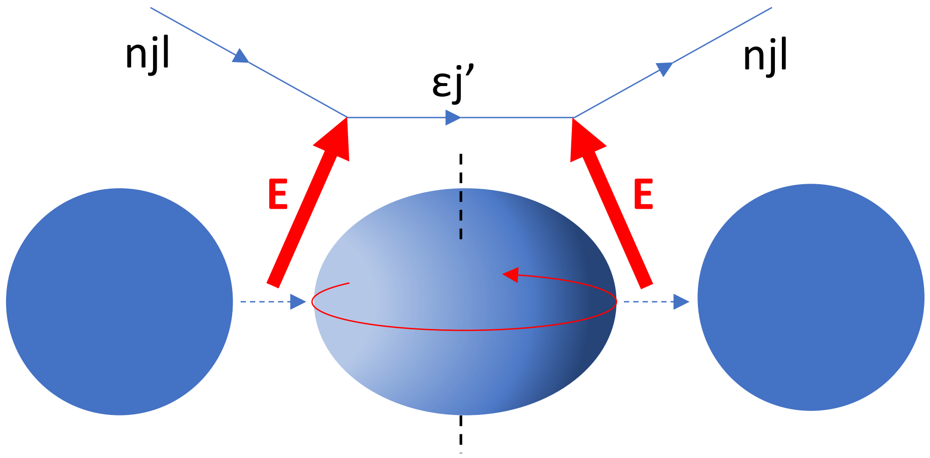

$$\Delta\varepsilon_{nlj} = -\frac{5\alpha}{4\pi} B(E2) \sum_{j'} (2j'+1) \begin{pmatrix} j' & j & 2 \\ \frac{1}{2} & -\frac{1}{2} & 0 \end{pmatrix}^2$$

$$\times \left(\int_{-\infty}^{-m_e} \frac{|\langle nl\,j|F_2|\varepsilon\, j'\rangle|^2 d\varepsilon}{\varepsilon - \varepsilon_{nl\,j} - E_{\mathrm{rot}}} + \int_{m_e}^{\infty} \frac{|\langle nl\,j|F_2|\varepsilon\, j'\rangle|^2 d\varepsilon}{\varepsilon - \varepsilon_{nl\,j} + E_{\mathrm{rot}}} \right),$$

$$E_{\mathrm{rot}} \approx \frac{2\pi^2}{9AR_0^4\beta_2^2}\ \mathrm{GeV\,fm}^4.$$

$$B(E2) \equiv B(E2; 2 \to 0) = \frac{1}{5}\left(\frac{3}{4\pi}\right)^2 Z^2 e^2 R_0^4 \beta_2^2.$$

Electric quadrupole contribution - Results

- Fitting function:

$$\frac{\Delta\varepsilon(Z,\Delta A)}{B(E2)} = [-\exp(\tilde{a}_0 + \tilde{a}_1 Z + \tilde{a}_2 Z^2) Z^{\tilde{a}_3} + \exp(\tilde{b}_0 + \tilde{b}_1 Z + \tilde{b}_2 Z^2) Z^{\tilde{b}_3} \Delta A] \frac{\text{meV}}{10^3\ \text{fm}^4},$$

- Radius variation:

$$\frac{\delta_R\varepsilon(Z)}{B(E2)} = \exp(\tilde{c}_0 + \tilde{c}_1 Z + \tilde{c}_2 Z^2) Z^{\tilde{c}_3} \frac{\text{meV}}{10^3\ \text{fm}^5},$$

	$1s$	$2s$	$2p_{1/2}$
$\tilde{a}_0$	-5.78	-10.3	-24.8
$\tilde{a}_1$	-8.74×10^{-3}	-1.10×10^{-2}	-1.92×10^{-2}
$\tilde{a}_2$	2.74×10^{-4}	3.36×10^{-4}	4.18×10^{-4}
$\tilde{a}_3$	3.41	3.46	5.70
$\tilde{b}_0$	-8.27	-12.7	-26.9
$\tilde{b}_1$	-1.59×10^{-2}	-1.80×10^{-2}	-2.33×10^{-2}
$\tilde{b}_2$	3.02×10^{-4}	3.64×10^{-4}	4.33×10^{-4}
$\tilde{b}_3$	2.81	2.85	4.96
$\tilde{c}_0$	-7.06	-11.5	-25.8
$\tilde{c}_1$	-1.54×10^{-2}	-1.78×10^{-2}	-2.51×10^{-2}
$\tilde{c}_2$	3.00×10^{-4}	3.64×10^{-4}	4.41×10^{-4}
$\tilde{c}_3$	3.52	3.57	5.75

Fitting + computation error < 12%

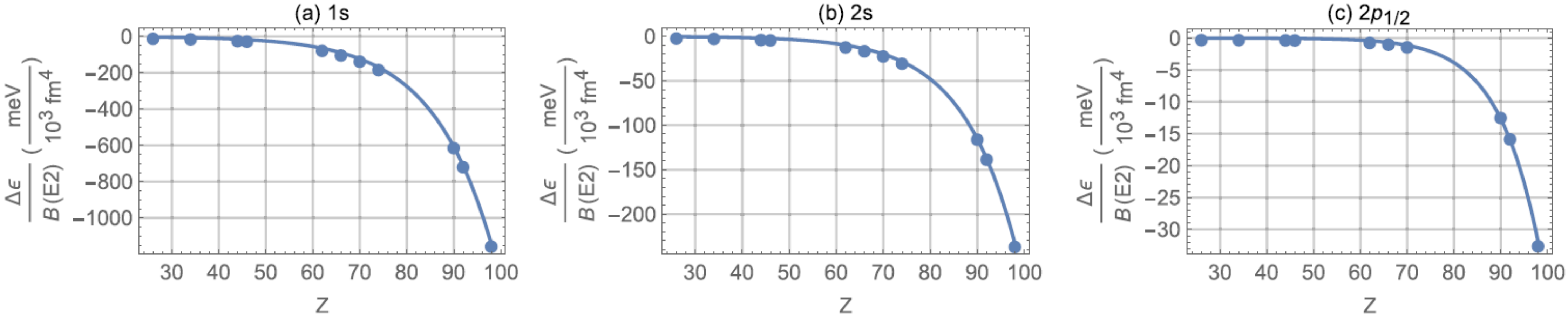

Effective potential for multielectron atoms

- Previous results for single-electron ions.
- Derive effective potentials → correct single-electron results.
- Potentials may be added to nuclear Coulomb potential in many-body codes.
- Long range polarization potential $V_L(r)$ with polarizability coefficient.
- Short range → cut off parameter b.

$$V_L(r)|_{r\to\infty} \to -\frac{e^2}{2}\frac{\alpha_0^{EL}}{r^{2L+2}}.$$

$$\alpha_0^{EL} = \frac{8\pi}{2L+1}\frac{B(EL;L\to 0)}{E_L}$$

Short-range behaviour

$$V_L(r) = -\frac{e^2}{2}\frac{\alpha_0^{EL}}{r^{2L+2}+b^{2L+2}}.$$

$$b = b(Z, A, R_0, \beta_2).$$

$$\Delta\varepsilon_\Psi^{(L)} = \langle\Psi|V_L|\Psi\rangle.$$

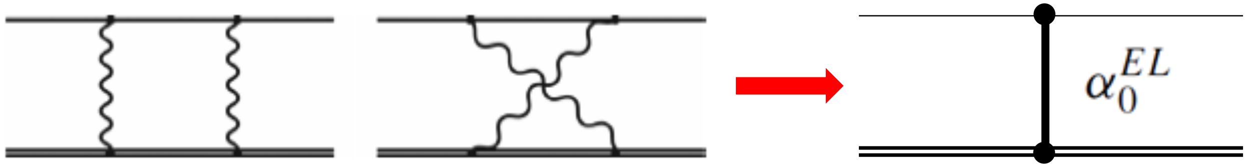

Effective potentials

$$V_1 = -\frac{1}{2}\frac{e^2\alpha_0^{E1}}{r^4 + b^4}, \quad \alpha_0^{E1} = \frac{8\pi B(E1)}{3E_{\mathrm{GR}}},$$

$$\begin{aligned} b(Z,A,R) = {} & [\exp(\lambda_0 + \lambda_1 Z + \lambda_2 Z^2)Z^{\lambda_3} \\ & + \exp(\nu_0 + \nu_1 Z + \nu_2 Z^2)Z^{\nu_3}\Delta A]\ \mathrm{fm} \\ & + \exp(\tau_0 + \tau_1 Z + \tau_2 Z^2)Z^{\tau_3}\delta R. \end{aligned}$$

$$V_2 = -\frac{1}{2}\frac{e^2\bar{\alpha}_0^{E2}}{r^6 + \tilde{b}^6}, \quad \bar{\alpha}_0^{E2} = \frac{8\pi}{5}\frac{B(E2)}{\bar{E}_{\mathrm{rot}}}, \quad \bar{E}_{\mathrm{rot}} = 50\ \mathrm{keV}$$

$$\begin{aligned} \tilde{b}(Z,A,R) = {} & [\tilde{\lambda}_0 + \tilde{\lambda}_1 Z + \exp(\tilde{\nu}_0 + \tilde{\nu}_1 Z + \tilde{\nu}_2 Z^2)\Delta A]\ \mathrm{fm} \\ & + \exp(\tilde{\tau}_0 + \tilde{\tau}_1 Z + \tilde{\tau}_2 Z^2)Z^{\tilde{\tau}_3}\delta R, \end{aligned}$$

- Values of all parameters are fitted from numerical calculation.
- Give correct single-electron contribution.
- Errors around 5%.
- These potentials are added to Coulomb potential and incorporated into many body calculations

Conclusion

- We studied the effects of electric nuclear polarization on electron energy-level shifts and isotope shifts.
- Effects are strongly enhanced in superheavy atoms.
- We consider contributions from nuclear giant electric-dipole resonance transitions (E1) and rotational transitions (E2).
- We derived effective potentials which model the corrections due to the nuclear polarizability → many-body calculation.
- Calculate nonlinearity in King's plot for isotope shifts → facilitate looking for new interactions beyond the Standard Model.

Radiative potential for QED corrections in many – electron atoms

Flambaum, Ginges PRA 722, 052115 (2005).

$$\Phi_{\text{rad}}(r) = \Phi_U(r) + \Phi_g(r) + \Phi_f(r) + \Phi_l(r) + \frac{2}{3}\Phi_{WC}^{simple}(r)$$

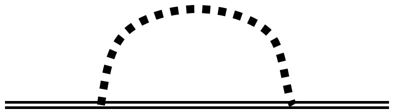

$\Phi_g(r)$ – magnetic formfactor
$\Phi_f(r)$ – electric formfactor
$\Phi_l(r)$ – low energy electric formfactor
$\Phi_U(r)$ – Uehling potential
$\Phi_{WC}(r)$ – Wichmann-Kroll potential

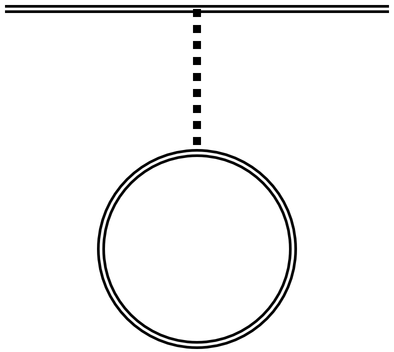

Ab initio calculation accuracy ~10 % for QED corrections to ns energy levels. To achieve 1%, $\Phi_f(r)$ and $\Phi_f(r)$ have free parameters which are chosen to fit QED corrections to the single-electron atom energies (Mohr, et al)

Use approximate, local radiative potential

$$\Phi_{\rm rad}(r) = \Phi_U(r) + \frac{2}{3}\Phi_{WC}^{\rm simple}(r) + \Phi_g(r) + \Phi_f(r) + \Phi_l(r)$$

- *Ab initio* derivation for $Z\alpha \ll 1$
- Refined to include higher orders in $Z\alpha$ by fitting to (Mohr *et al.*) Lamb shifts for high states in H-like ions for $10 \le Z \le 110$

e.g.

$$\Phi_f(r) = -A(Z,r)\frac{\alpha}{\pi}\Phi(r)\int_1^\infty dt\,\frac{1}{\sqrt{t^2-1}}\left[\left(1-\frac{1}{2t^2}\right)\left(\ln(t^2-1)+4\ln(1/Z\alpha+0.5)\right)-\frac{3}{2}+\frac{1}{t^2}\right]e^{-2trm}$$

$$\Phi_l(r) = -\frac{B(Z)}{e}Z^4\alpha^5 mc^2 e^{-Zr/a_B}$$

%-difference between our self-energy results and those of Mohr, Kim for H-like ions

Z	10	20	30	40	50	60	70	80	90	100	110
$5s_{1/2}$	0.0	0.4	0.5	0.3	0.0	-0.2	-0.2	0.0	0.1	0.1	0.0
$5p_{1/2}$	-0.8	-3.6	-2.8	-1.8	-1.1	-0.7	-0.3	0.1	0.8	1.8	3.3
$5p_{3/2}$	-2.5	-8.3	-8.9	-7.3	-5.2	-3.1	-1.1	0.4	1.4	1.7	0.8

QED radiative corrections: accuracy ~0.1% for s-levels. Includes many-body corrections. V.F. and Ginges. Phys. Rev. A 72, 052115 (2005).

Low-energy theorem is used to calculate QED radiative corrections to electromagnetic amplitudes

- Small parameter=E/ω

E=energy of valence electron=$10^{-5}\, mc^2$

ω–virtual photon frequency =mc^2

- Results are expressed in terms of self-energy Σ and $d\Sigma/dE$ (vertex, normalization)
- Radiative potential contribution: $\alpha^3 Z^2 \ln(\alpha^2 Z^2)$

Other contributions: $\alpha^3 (Z_i + 1)^2$, Z_i–ion charge

In neutral atoms (Z_i=0) radiative potential contribution is Z^2 times larger!

Thus, it is sufficient to add radiative potential to Coulomb potential in many body calculations of electromagnetic amplitudes and energy levels.

- Z=55 Cs atom: Total QED correction to parity violating amplitude E_{PV}= -0.41%(weak)+0.43%(E1)-0.34%(δE)=-0.32%
- To avoid misunderstanding: our radiative potential method is not suitable for calculation of radiative corrections for operators localized at distance smaller than electron Compton wavelength (e.g. weak interaction) since operator $\Sigma(r, r',E)$ is non-local there.
  Radiative potential may give poor accuracy for electromagnetic amplitudes when $Z_i \sim Z$

Spectra, hyperfine structure, electromagnetic amplitudes and isotope shifts up to Z=120

- Radiative potential and calculations of QED radiative corrections to energy levels and electromagnetic amplitudes in many-electron atoms. Flambaum, Ginges, PRA 72, 052115 (2005).
- Many body perturbation theory combined with configuration-interaction. **Efficient for many electrons in open shells!**
  Dzuba,Flambaum, Kozlov, PRA 99, 032501 (2019) - 2022
- **If we add calculated isotope shifts to measured atomic spectra of neutron-deficient isotope produced in laboratory,** $E=E_0 + IS$, **we predict spectra of neutron-rich isotopes near island of stability which may be searched in astrophysical data.**
  spectra of Es Z=99 from a star observed (?)
  Flambaum,Geddes,Viatkina, Isotope shift, non-linearity of King plot and search for new particles, PRA 97, 032510 (2018)

Field shift

single-electron mean-field approximation

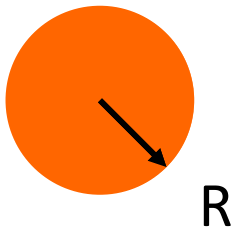

Uniformly charged spherical nucleus

Perturbation

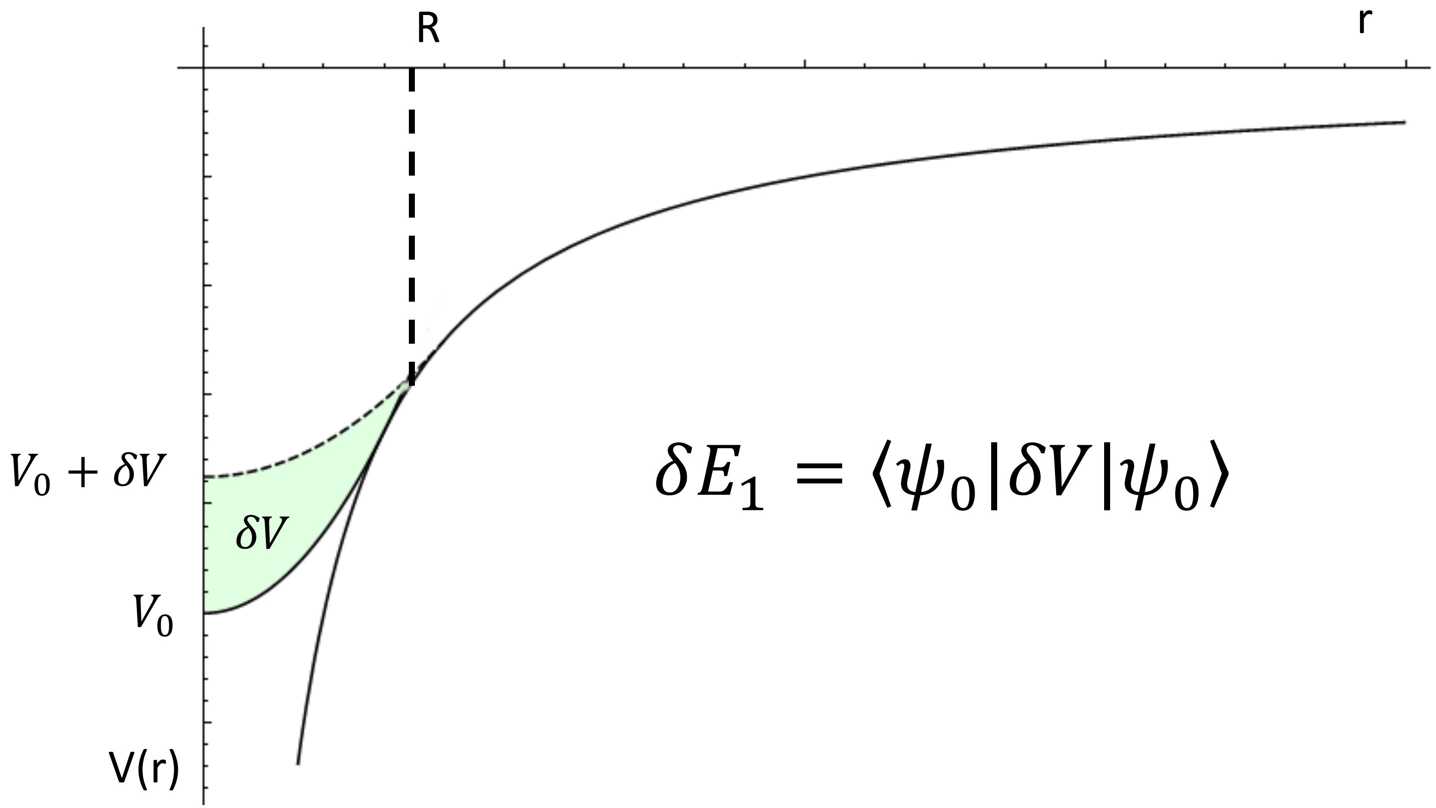

$$\delta E_1 = \langle \psi_0 | \delta V | \psi_0 \rangle$$

Mass shift

Energy difference between the infinite and finite mass isotopes:

$$\Delta E_{\infty,M} = \boxed{\frac{\langle \sum_i p_i^2 \rangle}{2(M+m)}} + \boxed{\frac{\langle \sum_{i>j} \mathbf{p}_i \mathbf{p}_j \rangle}{(M+m)}}$$

NMS: change of the reduced mass
(single-electron effect)

SMS: electron correlations
(many-electron effect)

(M – nuclear mass, m – electron mass, p – electron momenta)

Mass shift

Energy difference between the infinite and finite mass isotopes:

$$\Delta E_{\infty,M} = \frac{K}{(M+m)}$$

$$\Delta E_{M_1,M_2} = \frac{K(M_1 - M_2)}{(M_1+m)(M_2+m)} \approx K\mu \qquad , m \ll M$$

$$\mu = \frac{1}{M_1} - \frac{1}{M_2}$$

(M – nuclear mass, m – electron mass, p – electron momenta)

Isotope shift, non-linearity of King plot and search for new particle Flambaum,Geddes,Viatkina, PRA 97, 032510 (2018)

							Nonlinearity (Hz)		
Ion	Z	A	A_1	A_2	A_3	Pair of transitions	Higher waves	Polarizability	Many-body
Ca^+	20	40	42	44	48	$3p^6 4s\ ^2S_{1/2} \rightarrow 3p^6 3d\ ^2D_{3/2}$	3.0×10^{-4}	-6.6×10^{-2}	$\pm 2.7 \times 10^{-3}$
						$3p^6 4s\ ^2S_{1/2} \rightarrow 3p^6 3d\ ^2D_{5/2}$			
Sr^+	38	84	86	88	90	$4p^6 5s\ ^2S_{1/2} \rightarrow 4p^6 4d\ ^2D_{3/2}$	1.1×10^{-2}	-2.6	± 0.25
						$4p^6 5s\ ^2S_{1/2} \rightarrow 4p^6 4d\ ^2D_{5/2}$			
Ba^+	56	132	134	136	138	$5p^6 6s^1\ ^2S_{1/2} \rightarrow 5p^6 5d\ ^2D_{3/2}$	-3.9×10^{-2}	7.4	∓ 1.9
						$5p^6 6s^1\ ^2S_{1/2} \rightarrow 5p^6 5d\ ^2D_{5/2}$			
Yb^+	70	168	170	172	176	$4f^{14} 6s\ ^2S_{1/2} \rightarrow 4f^{13} 6s^2\ ^2F^o_{7/2}$	-3.1	39	± 12130
						$4f^{14} 6s\ ^2S_{1/2} \rightarrow 4f^{14} 5d\ ^2D_{3/2}$			
						$4f^{14} 6s\ ^2S_{1/2} \rightarrow 4f^{14} 5d\ ^2D_{3/2}$	3.1	-18	± 386
						$4f^{14} 6s\ ^2S_{1/2} \rightarrow 4f^{14} 5d\ ^2D_{5/2}$			
Hg^+	80	196	198	200	204	$5d^{10} 6s\ ^2S_{1/2} \rightarrow 5d^9 6s^2\ ^2D_{3/2}$	3.0	-13	± 2382
						$5d^{10} 6s\ ^2S_{1/2} \rightarrow 5d^9 6s^2\ ^2D_{5/2}$			

If we have an extra term

$$\nu_a = F_a \delta\langle r^2\rangle + K_a\mu + G_a\gamma$$

$$\nu_b = F_b \delta\langle r^2\rangle + K_b\mu + G_b\gamma$$

(G is electron structure factor, γ is nuclear factor) then

$$\tilde{\nu}_a = \frac{F_a}{F_b}\tilde{\nu}_b - \frac{F_a}{F_b}K_b + K_a + G_b\frac{\gamma}{\mu}\left(\frac{F_a}{F_b} - \frac{G_a}{G_b}\right)$$

source of non-linearity.

This term vanishes if $F_a/F_b=G_a/G_b$ (similar transitions),
e.g. in Yb^+ we have $6s\text{-}5d_{3/2}$ and $6s\text{-}5d_{5/2}$ transitions
(Counts et al, PRL **125**, 123002 (2020)).
Field Isotope Shift is dominated by 6s and non-linearity is small, ~ 10^{-6}.

Parity and time reversal violating nuclear polarization

- atomic Electric Dipole Moment due to nuclear T,P-odd polarizability.
- electric + magnetic vertices instead of 2 electric vertices for usual polarisabilty
- We studied this → electron EDM experiments are sensitive to hadron CP-violation, theta-term, axion dark matter, etc.
- Nuclear spin may be zero as in electron EDM experiments

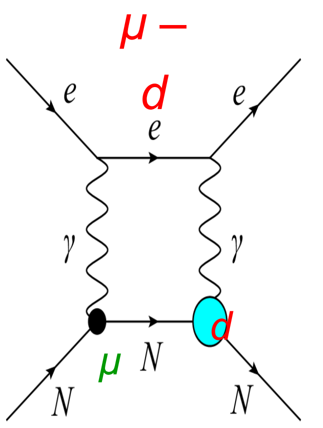

Internal nuclear excitations

	^{232}ThO	^{180}HfF$^+$
$\lvert C_{SP}\rvert$	7.3×10^{-10} [31]	1.8×10^{-8} [29, 53]
$\lvert d_p\rvert$	$1.1\times10^{-23} e\cdot\text{cm}$	$1.5\times10^{-22} e\cdot\text{cm}$
$\lvert d_n\rvert$	$1.0\times10^{-23} e\cdot\text{cm}$	$2.0\times10^{-22} e\cdot\text{cm}$
$\lvert\bar g^{(0)}_{\pi NN}\rvert$	3.1×10^{-10}	5.6×10^{-9}
$\lvert\bar g^{(1)}_{\pi NN}\rvert$	3.3×10^{-10}	8.2×10^{-9}
$\lvert\tilde d_d\rvert$	$9.3\times10^{-25}\text{cm}$	$2.2\times10^{-23}\text{cm}$
$\lvert\tilde d_u\rvert$	$1.7\times10^{-24}\text{cm}$	$5.8\times10^{-23}\text{cm}$
$\lvert\bar\theta\rvert$	1.4×10^{-8}	2.7×10^{-7}

$\frac{\lvert\xi_p\rvert}{10^{-23}\text{cm}}$	$\frac{\lvert\xi_n\rvert}{10^{-23}\text{cm}}$	$\frac{\bar g^{(0)}_{\pi NN}}{10^{-9}}$	$\frac{\bar g^{(1)}_{\pi NN}}{10^{-9}}$	$\frac{\bar g^{(2)}_{\pi NN}}{10^{-9}}$	$\frac{\tilde d_u}{10^{-24}\text{cm}}$	$\frac{\tilde d_d}{10^{-24}\text{cm}}$	$\frac{\bar\theta}{10^{-8}}$
2.2	3.0	2.9	0.6	1.5	2.1	1.9	9

Limits on $\xi_{p,n}$, $\bar g^{(0,1,2)}_{\pi NN}$, $\tilde d_{u,d}$ and $\bar\theta$ obtained from the ThO limit on $\lvert C_{SP}\rvert < 7.3\times10^{-10}$.

V.V. Flambaum, J.S.M. Ginges, G. Mititelu, arXiv:nucl-th/0010100 (2000)
V.V. Flambaum, M. Pospelov, A. Ritz, and Y.V. Stadnik, PRD 102, 035001 (2020)
V.V. Flambaum, I.B. Samsonov, H.B. Tran Tan, JHEP 2020, 77 (2020)
V.V. Flambaum, I.B. Samsonov, H.B. Tran Tan, PRD 102, 115036 (2020)